

Autonomous Volume Transitions of a Polybase Triblock Copolymer Gel in a Chemically Driven pH-Oscillator

Paul D. Topham,^{*1} Jonathan R. Howse,² Colin J. Crook,¹ Anthony J. Gleeson,³ Wim Bras,⁴ Steven P. Armes,¹ Richard A. L. Jones,² Anthony J. Ryan¹

¹ Department of Chemistry, University of Sheffield, Sheffield S3 7HF, UK.
Email: p.topham@sheffield.ac.uk

² Department of Physics and Astronomy, University of Sheffield, Sheffield S3 7RH, UK.

³ CCLRC Daresbury Laboratory, Warrington, WA4 4AD, UK.

⁴ DUBBLE CRG, ESRF, 6 rue Jules Horowitz, BP 220, F-38043 Grenoble Cédex 9, France.

Summary: A pH-responsive ABA triblock copolymer, comprising poly(methyl methacrylate)-*block*-poly(2-(diethylamino)ethyl methacrylate)-*block*-poly(methyl methacrylate) [PMMA-*b*-PDEA-*b*-PMMA], has been cast into thin films with a well-defined microstructure. Small Angle X-ray Scattering (SAXS) and Atomic Force Microscopy (AFM) studies confirm that this copolymer forms a hydrogel consisting of PMMA spheres embedded within a polybase PDEA matrix, with the PMMA domains acting as physical cross-links. The hydrogel has a pH-reversible coil-globule transition at around pH 4.5. This responsive physical property was exploited by immersing a sample of copolymer hydrogel in an aqueous solution containing a cyclic pH-oscillating reaction, whereby the pH was continuously oscillated above and below the transition pH so as to induce autonomous volume transitions. The changes in microscopic and macroscopic length scales correlate closely during (de)swelling cycles, with affine behaviour occurring over five orders of magnitude.

Keywords: Polybase, pH-responsive, triblock copolymer, SAXS, poly(2-(diethylamino)ethyl methacrylate)

Introduction

The search for an entirely synthetic working molecular machine has been on-going over many years.¹⁻⁴ Naturally-occurring nanoscale machines found in cell biology operate by converting chemical energy into mechanical energy at very high levels of efficiency. A device that performs this type of energy conversion at the molecular level is often referred to as a *molecular motor*. The basis of such molecular motors is a conformational change of a responsive macromolecule, and in biological systems the polymer is also active in that it acts as the catalyst for the reaction releasing the chemical energy. Non-catalytic passive conformational changes can also be used to make molecular motors based on simple

stimulus-responsive units, such as in synthetic polymers that respond to, but do not take part in, the driving chemical reaction. An example of this would be the coil-to-globule transition⁵ of a polyelectrolyte, coupled with a pH-oscillating reaction, that exhibits controlled volume pulsations that can exert an external force.⁶ An additional advantage conferred by using complementary pairs of polyacids and polybases is that devices fabricated from these two building blocks can be efficiently bipolar such that one polymer exhibits a positive response while the other simultaneously exhibits a negative response. For example, one polymer may be swollen while the other is collapsed for a given solution pH. In principle, judicious selection of the respective pK_a values should enable a polyacid and a polybase to be used in tandem. At low pH, both of the polyelectrolytes are protonated, so the polyacid is charge-neutral and the polybase exists as cationic polyelectrolyte. The charge density on the polybase chains induces both chain expansion and also mutual electrostatic repulsion between neighbouring chains, whereas the polyacid chains, which are uncharged and hydrophobic, remain in their collapsed conformation. At high pH, the polybase chains become charge-neutral and collapse, whereas the polyacid chains ionize and hence expand as anionic polyelectrolytes.

For an aqueous solution containing a binary mixture of a polyacid homopolymer and a polybase homopolymer, these two components would simply dissolve in or precipitate from solution as they experienced favourable and unfavourable solvent conditions. In order to generate a force, an external system (i.e. a load) must be mechanically coupled directly to the polymers. One method of coupling (and amplifying) this response is to synthesize a polymer gel of each polyelectrolyte. The macroscopic behaviour of the gel is then the product of the individual molecular conformational changes. To ensure that the polymer gel remains intact during any induced oscillations, it is essential to incorporate crosslinks to the material. Although chemical crosslinks can provide structural integrity, this approach inevitably introduces spatial inhomogeneities in crosslink density which lead to locally anisotropic expansion and contraction, creating mechanical stresses throughout the network.⁷ Such inhomogeneous stresses ultimately lead to mechanical failure of the gel. This problem can be overcome by introducing physical crosslinks to create a polymer network with a *homogeneous* crosslink density distribution. Annealed physical crosslinks allow isotropic expansion, thus minimizing the stresses induced during volume transitions. One method to introduce such physical crosslinks is to use block copolymer self-assembly to induce microphase separation.^{8, 9} This strategy requires at least two immiscible polymers, which are covalently attached to one another. When

allowed to equilibrate by diffusion (during annealing), the block copolymer chains undergo microphase separation into distinct nano-scale domains of the two individual blocks, while remaining chemically bound to each domain. More specifically, by controlling the composition of a symmetrical ABA triblock copolymer, one can generate physically crosslinked networks with a desired microstructure, such as lamellae, cylindrical rods or spheres.¹⁰

A further advantage of using physical crosslinking, compared to chemical crosslinking, is that the spatial location of the crosslinks can be monitored by small angle x-ray scattering (SAXS)¹¹ since the electron density differences between the individual blocks will often provide sufficient x-ray contrast. This allows a direct correlation between changes in length scales at the molecular level and the changes in macroscopic length scales (as measured by optical microscopy) within the gel. If the overall macroscopic volume change relates directly to the summation of many small volume changes at the molecular level, gel expansion is described as being *affine*¹². In principle, such a device should function effectively at all intermediate length scales down to a single unit consisting of a single copolymer chain.

Previously¹³ we have reported autonomous, affine volume transitions of a polyacid triblock copolymer gel¹⁴ in a chemically driven pH-oscillator, referred to as a Landolt Oscillator.¹⁵ The polymer comprised a central pH-responsive poly(methacrylic acid) [PMAA] block and two outer poly(methyl methacrylate) [PMMA] blocks that act as glassy, hydrophobic physical crosslinks. The Landolt pH-oscillator system is ideally suited to PMAA, whose pK_a value lies around pH 5.5 (the exact pK_a value depends on the molecular weight, structure and copolymer components¹⁶⁻¹⁸), because the reaction solution exhibits sustained oscillations between pH 3 and pH 7 in a continuously fed and stirred reactor. However, when a polybase triblock copolymer, poly(methyl methacrylate)-*block*-poly(2-(diethylamino)ethyl methacrylate)-*block*-poly(methyl methacrylate) [PMMA-*b*-PDEA-*b*-PMMA], was placed in the same Landolt pH-oscillator reaction solution, it did not undergo the expected autonomous volume transitions. Unfortunately, a side-reaction occurred between the pendent tertiary amine groups on the PDEA chains and the ferrocyanide ions present in the solution that prevented reversible protonation; indeed, the formation of permanently bound ligands was observed by IR spectroscopy. Herein we report the use of a related permanganate-based pH-oscillatory system¹⁹ to drive the autonomous volume transitions in PMMA-*b*-PDEA-*b*-PMMA. Prior to dynamic studies on the PMMA-*b*-PDEA-*b*-PMMA triblock copolymer, we also carried out a static pH

study to identify the critical pH for the coil-to-globule transition and to assess whether or not this physically cross-linked polybase triblock copolymer would be a suitable counterpart to the PMMA-*b*-PMAA-*b*-PMMA copolymer. When a sample of this polybase hydrogel is immersed in a solution, the mean separation between the spherical PMMA domains will depend on the solution pH, as shown in Figure 1.

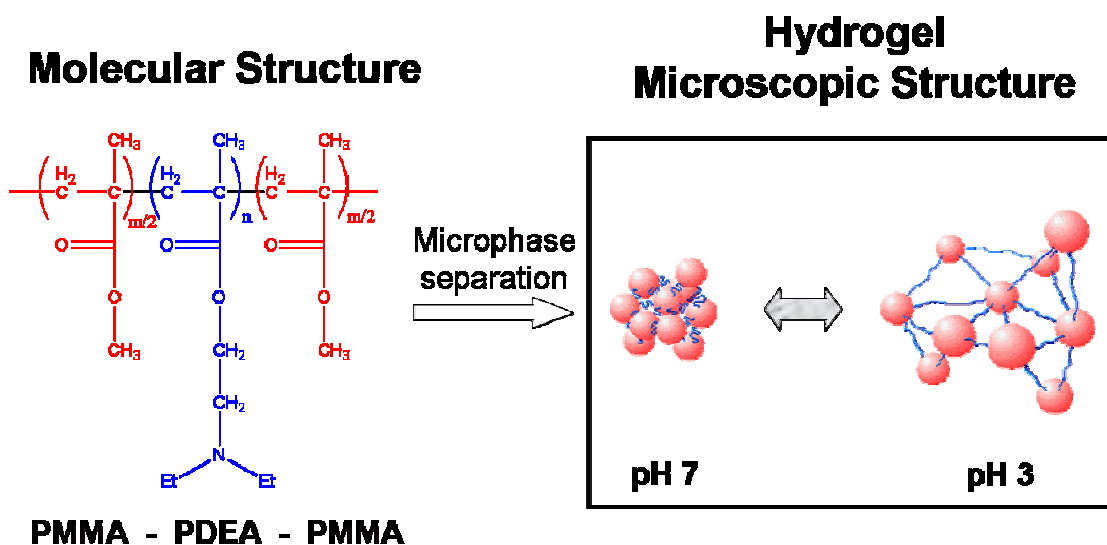


Figure 1. Schematic diagram of the structure of the polybase triblock copolymer, poly(methyl methacrylate)-*block*-poly(2-(diethylamino)ethyl methacrylate)-*block*-poly(methyl methacrylate) [PMMA-*b*-PDEA-*b*-PMMA]. The microscopic structure (right) shows an illustration of the “*pseudo*” unit cell (after microphase separation) either side of the coil-globule transition.

Experimental

Materials. All materials were purchased from Aldrich. Sodium sulfite (98%), sodium bromate (99+%), potassium permanganate (99+%) and perchloric acid (70% aqueous solution) were used as received. The synthesis of poly(methyl methacrylate)-*block*-poly(2-(diethylamino)ethyl methacrylate)-*block*-poly(methyl methacrylate) (PMMA-*b*-PDEA-*b*-PMMA) triblock copolymer via Group Transfer Polymerization (GTP) is described elsewhere.²⁰ Size Exclusion Chromatography (SEC) revealed that the polymer had a number-average molecular weight, M_n , of 182 kg mol⁻¹ and a polydispersity, PD, of 1.12. The PMMA volume fraction was found to be 0.17 using ¹H-NMR and density measurements.

Film Casting. The triblock copolymer was dissolved in THF (40% w/w solution) and a doctor blade was used to cast films of desired thicknesses onto PTFE sheets. The solvated

copolymer samples were then placed in a desiccator with a THF-rich environment where a small aperture allowed the slow release of THF vapour. This treatment resulted in slow evaporation of THF from the films over 168 h, allowing sufficient time for optimised microphase separation of the copolymer, in order to attain an equilibrium structure.

Static pH experiment. To recreate the conditions experienced during pH oscillations triblock copolymer gels were swollen to equilibrium in aqueous solutions obtained from the spent permanganate dynamic oscillatory system (> 99 %) adjusted from pH 2 to pH 7 using H₂SO₄ and NaOH stock solutions. Using such solutions directly from the dynamic pH oscillating reaction ensured that the ionic strength was approximately constant at around 0.07. The solutions were divided into two in order to have two copolymer samples for each pH value. Pre-weighed samples of the triblock copolymer were placed into each solution for 72 h to ensure that equilibrium swelling had been attained. The solution pH was recorded prior to SAXS and mass analysis in order to monitor any pH drift that occurred as a result of interaction between the copolymer and the solution. Each piece of gel was carefully removed from its solution and weighed. Excess solution was dried from the external surface of each gel prior to gravimetric analysis. The copolymer was then re-immersed in the aqueous solution to ensure that equilibrium was maintained before SAXS was used to analyze the microscopic changes in length scales. SAXS patterns were recorded for each sample on Station 16.1 at Daresbury Scientific Laboratories, where each piece of copolymer was irradiated for 30 seconds while encapsulated in Kapton tape to prevent the loss of any solution from the interior of the polymer. The station specifications have been detailed elsewhere.²¹

pH-oscillating reaction. Sodium sulfite (236 mM), sodium bromate (250 mM), potassium permanganate (2.0 mM) and perchloric acid (33 mM) solutions were made up in separate 1 L volumetric flasks using deionized water. The ionic strength of the oscillating solution that provided the optimized pH cycles was calculated to be 0.13 (which is approximately twice the ionic strength of the oscillating solution used for the static pH experiment). Once fully dissolved, the components were pumped into a continuously stirred tank reactor (CSTR), at a rate of 4.0 ml min⁻¹ (total solution) giving an average residence time of 12.5 minutes. The vessel was equipped with four windows (two were optically transparent and two were x-ray transparent) and an outlet pipe to allow drainage of waste materials as the fresh reactants are supplied (see Figure 2). An external water bath, held at 60 °C, was used to pump water around a glass heat exchange pipe situated in the vessel. The oscillatory system used here has an optimum working

temperature of 45 °C. A pH probe was held in the vessel and the resulting pH data was recorded on a computer. A pre-cast copolymer sample was held in the solution using tweezers and its progress was monitored by optical microscopy (macroscopic) and SAXS (microscopic) on BM26 (DUBBLE) at the European Synchrotron Radiation Facility (ESRF). The ESRF beam line optics and construction are detailed elsewhere.²² A “real” image of the gel was recorded every minute and its length measured (“tweezers-to-end of gel” distance) using an automated vision assistant script from the Labview 7.1 software package. 2D SAXS frames were captured every 120 seconds throughout the experiment. An illustration of the experimental set-up is shown in Figure 2.

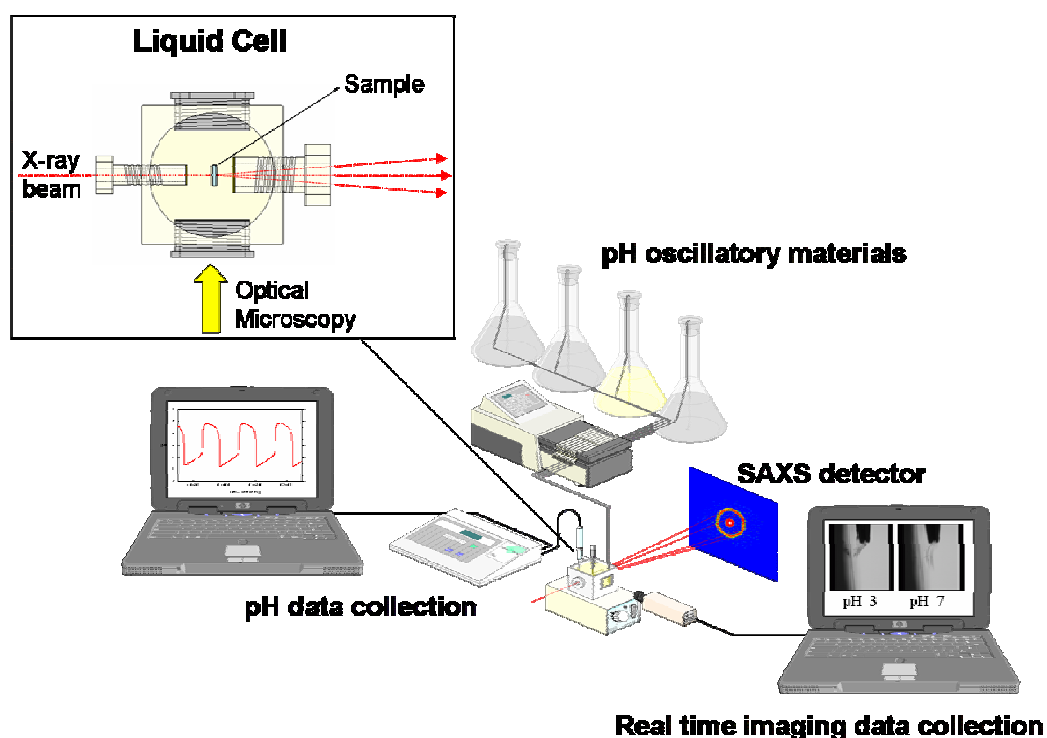


Figure 2. Experimental set-up for the dynamic pH studies.

Results/ Discussion

Static pH experiment. After 72 h immersed in solution, the static samples were enveloped in Kapton and analyzed by SAXS. The 2D SAXS patterns were radially integrated (360°) to give 1D data of x-ray intensity versus q , plotted in Figure 3. The pH ranged from ~ 2 (bottom trace) up to ~ 7 (upper trace). The scattering patterns are translated along the intensity axis for clarity.

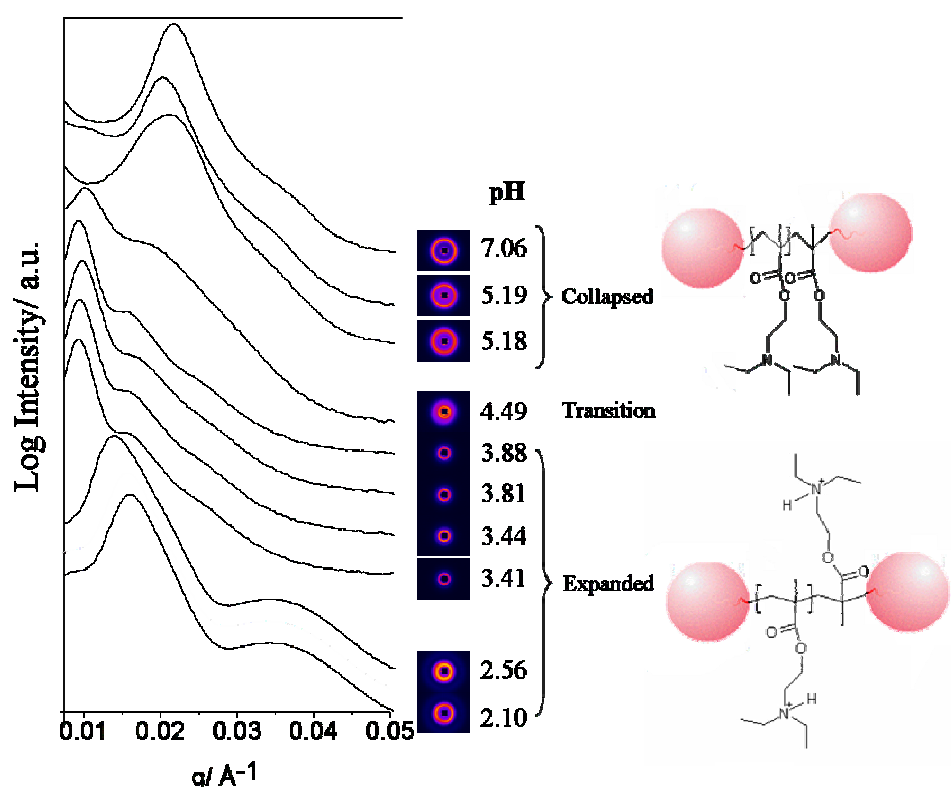


Figure 3. Plot of the 1D SAXS data (log Intensity against q) for samples of PMMA-*b*-PDEA-*b*-PMMA hydrogel subjected to 72 hours at different pH. Each trace has been translated along the intensity axis for ease of viewing. The 2D SAXS patterns (and pH values) are featured to the right of their corresponding 1D trace and two illustrations of the molecular activity at the two pH extremes are included. The large spheres represent the PMMA aggregates that link many (~ 200) PDEA chains together.

Above pH 5, the triblock copolymer chains are collapsed and produce an intense SAXS peak at high q ($\sim 0.022 \text{ \AA}^{-1}$), indicating that the PMMA clusters are relatively close together (d-spacing $\sim 286 \text{ \AA}$). At pH 4.5, there are two distinct spatial regimes; a collapsed

interior and an expanded exterior (indicated by two SAXS structural features at $q \sim 0.010$ and ~ 0.018), as this pH corresponds approximately to the coil-globule transition of the PDEA chains. Below pH 4 the polymer gel is in the expanded state and the scattering pattern comprises a peak in the structure factor associated with the average separation of the PMMA spheres ($\sim 650 \text{ \AA}$) and a series of higher q features that could be due to higher order reflections or even the form factor of the spheres.

Interestingly, the pK_a at which the coil-globule transition is observed is significantly lower than that of linear PDEA homopolymer ($< 25 \text{ kg mol}^{-1}$), which has been determined to be around pH 7 by acid titration in aqueous solution.²³ This difference is most likely due to the much higher local concentration of the PDEA chains, which means that this material is harder to protonate (i.e. resists the build-up of cationic charge density) and therefore acts as a much weaker polybase. There are a number of features of tethered macromolecular systems that could lead to the pK_a being lower than that observed in low molar mass polymers, it could be attributed to the higher molecular weight of our material, the physical crosslinks and/ or the presence of hydrophobic PMMA constituents, which increase the general hydrophobicity of the gel.^{24, 25} Moreover we have also recently observed a large decrease in the pK_a of PDEA brush,¹⁴ formed by a grafting-from technique,²⁶ and an increase in the pK_a of polyacid brushes¹⁴ where the shift is most likely attributed to crowding in the dry-brush regime, where a bigger chemical potential is required to create a charge on a polyelectrolyte in an already highly charged environment.

Below pH 4.0 the gels are extensively protonated and hence expanded, with additional SAXS peaks indicating higher order structure within the swollen gel. Below pH 2.6, there is some electrostatic screening^{16, 27} between adjacent chains, inducing partial contraction of the PDEA matrix.

To illustrate the static pH-dependence of the PMMA-*b*-PDEA-*b*-PMMA triblock copolymer more clearly, the expansion ratio (both mass and volume) was calculated for each sample using equations 1.1 and 1.2:

$$\text{Mass Expansion Ratio} = \frac{m_f - m_0}{m_0} \quad (1.1)$$

$$\text{Volume Expansion Ratio} = \frac{d_f^3 - d_0^3}{d_0^3} \quad (1.2)$$

Where m_f is the final mass, m_0 the pre-weighed dry mass, d_f the final d-spacing between the PMMA aggregates and d_0 the original dry d-spacing of the copolymer sample. The SAXS d-spacing, determined from the position of the peak position in a Percus-Yevick structure factor,²⁰ has been converted into a volume (yielding a *pseudo* unit cell of Å³ dimensions) in order to compare expansion ratios, as shown in Figure 4.

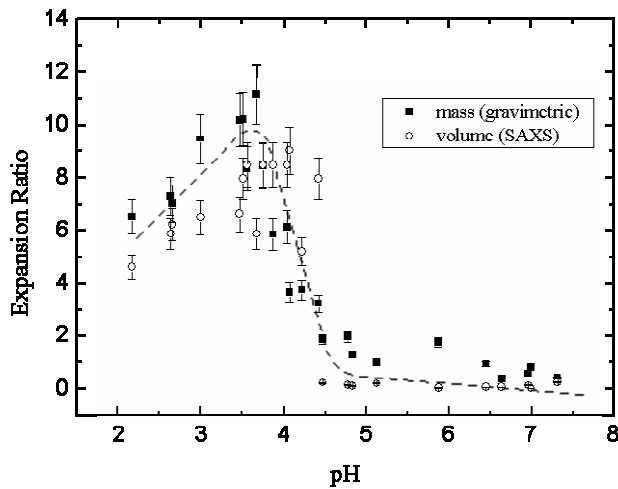


Figure 4. Plot of the expansion ratio against pH as measured by mass increase and SAXS (volume increase). The dashed line is a guide to the eye.

It is clear from the expansion ratios shown in Figure 4 that there is a close correlation between the mass of aqueous solution accommodated during swelling and the volume increase between the hydrophobic PMMA domains within the network. The mass ratios are generally higher than the corresponding volume ratios, which we attribute to the

presence of excess solution on the exterior surface of the gels and some interstitial swelling at grain boundaries in the ordered block copolymer. This additional solution increases the mass of a given sample but will not increase the separation between the hydrophobic domains. The data points where the volume appears higher than the mass is during the transition period, whereby the q value for the most intense peak was used (at lower q). Figure 4 further indicates classical polyelectrolyte behavior,^{16, 25, 27-29} with the ionic screening effect apparent at low pH, as a substantial decrease in mass and volume is observed. Above pH 4.5, the gels are collapsed, whereas below pH 4 the gels are expanded. Between pH 4 and 4.5, the gel goes through its coil-to-globule transition whereby part of the PDEA matrix is protonated and the other part is charge neutral. Gels over this pH range displayed a contracted central core with an expanded exterior. According to these data, oscillating the pH of the aqueous solution in which a PDEA-based triblock copolymer is immersed above and below pH 4.5 by at least one pH unit leads to autonomous volume transitions of the copolymer gel as it accommodates/ expels its surrounding solution; these volumetric transitions can be monitored by SAXS.

Dynamic pH-experiment. The pH-oscillating experiment was set up (Figure 2) and an 80 μm thick sample of PMMA-*b*-PDEA-*b*-PMMA was placed in the path of the x-ray beam. Optical microscopic images and x-ray data were collected periodically for 7 complete pH cycles. During each oscillation, the pH remains above pH 4.5 for 25 minutes and below this pH for 30 minutes, which allows sufficient time for the gel to significantly change conformation. Figure 5 shows the pH, the macroscopic length and the microscopic length of the polymer sample during the experiment (the q^* values, in \AA^{-1} , have been converted to a d-spacing value, in \AA).

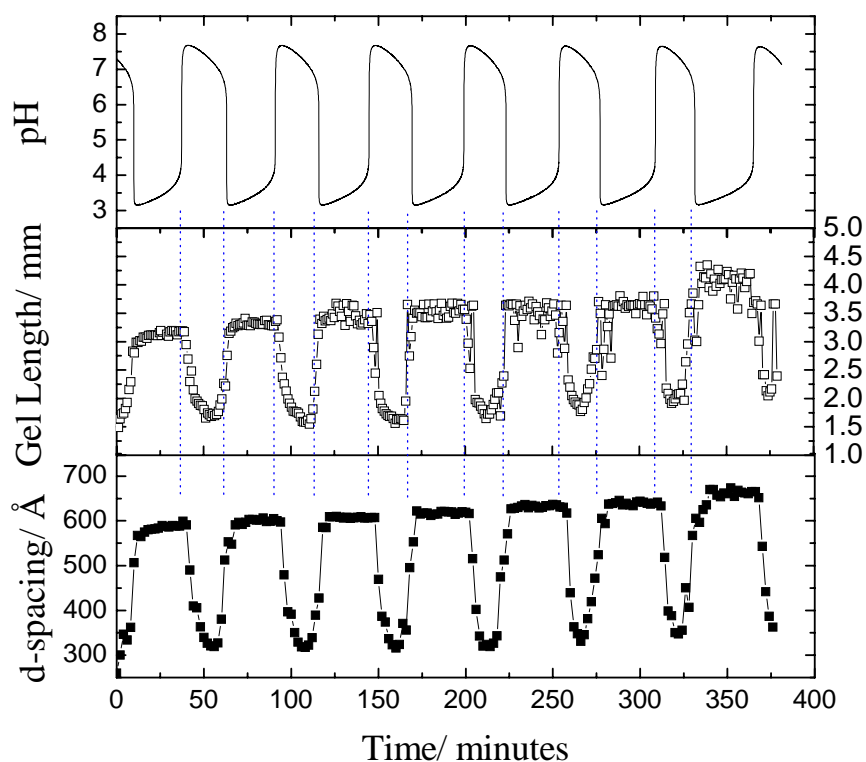


Figure 5. Plot of the pH trace (top), macroscopic data (middle) and microscopic SAXS data (bottom) during the pH-oscillation reaction. The dashed lines indicate the time at which the environment pH switches either above or below 4.5.

The data clearly illustrate that an 80 μm thick PMMA-*b*-PDEA-*b*-PMMA triblock copolymer gel exhibits seven continuous volume transitions as the pH oscillates between 3 and 8. When the solution is acidic, the copolymer expands as the PDEA chains become protonated and hydrophilic, accommodating the surrounding aqueous solvent. As the pH shifts to neutral, there is an incubation period whereby the copolymer gel remains swollen before the PDEA chains become deprotonated (and hydrophobic) and the copolymer chains contract. This delay in contraction is attributed to the slower diffusion process of expelling solvent molecules compared to accommodating them. Similar hysteresis effects have been recently observed for PDEA microgel particles.³⁰ The microscopic length scale changes appear to closely match the macroscopic length scale changes. To show this more

clearly, the length data has been converted to a percentage expansion using equation 1.3 and is shown in Figure 6.

$$\text{Expansion (\%)} = \frac{l_t - l_0}{l_0} \times 100 \quad (1.3)$$

l_t is the characteristic length of the copolymer gel (from both micro- and macroscopic) at time t and l_0 the original dry length at the start of the experiment.

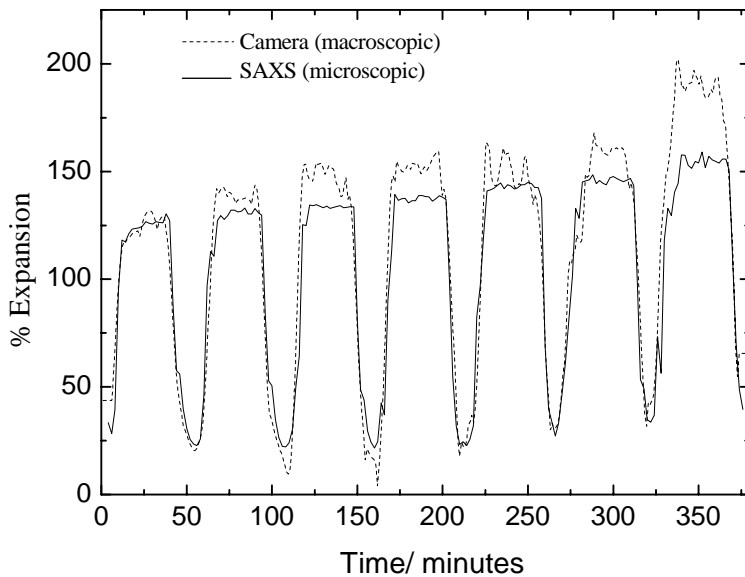


Figure 6. Plot of the micro- and macroscopic percentage expansion against time.

The data sets follow each other very closely during the volume transition steps and whilst the gel is collapsed. However, when the gel is expanded, the data sets diverge somewhat after the first pH cycle. This is because the triblock copolymer gel begins to tear during the second expansion, causing the end of the gel to be further from the tip of the tweezers at the extremes of each expansion. Tearing occurred at the point where the tweezers were holding the gel in place. Within the clamp, the polymer did not experience the surrounding solution changes, whereas just outside the tweezers the polymer exhibited the full range of volume changes. As a result, significant stress was introduced to the

sample, causing it to fracture. During this tearing process, anomalously high data points are recorded because the macroscopic data was obtained using an automated software package which measured the distance from the tip of the tweezers to the very end of the gel sample. Conversely, the SAXS peak comes from regions where the scattering centers are highly correlated so it essentially ignores any macroscopic physical defects. Taking these macroscopic defects into account, the coil-to-globule transition of the PMMA-*b*-PDEA-*b*-PMMA triblock copolymer exhibits molecular shape changes over five orders of magnitude in length scales, and mirrors the affine volume changes previously demonstrated with analogous PMMA-*b*-PMAA-*b*-PMMA copolymer gels.¹³

Conclusion

We have demonstrated that PMMA-*b*-PDEA-*b*-PMMA triblock copolymer gels exhibit a reversible coil-globule transition at around pH 4.0 – 4.5, which is much lower than the pK_a reported for PDEA homopolymer.²³ Autonomous volume transitions of such copolymer gels were observed over seven oscillatory pH cycles, with a typical macroscopic collapsed gel length of 1.5 mm and an expanded length of 3.5 mm. The corresponding microscopic lengths varied between 325 Å (collapsed) and 650 Å (swollen) and the macro- and microscopic data are closely correlated, indicating isotropic expansion of the material and affine behaviour. In principle this means that one can reduce the dimensions of such smart materials to as low as the pseudo unit cell to obtain pH-responsive volume transitions capable of exerting an external force.

Acknowledgement

This work was supported by ICI PLC and the EPSRC; grant numbers GR/R77544 (PDT), GR/S47496 (JRH), GR/R74383 (CJC). SPA is the recipient of a five-year Royal Society-Wolfson Research Merit Award.

1. Yoshida, R.; Kokufuta, E.; Yamaguchi, T. *Chaos* **1999**, 9, (2), 260-266.
2. Yoshida, R.; Sakai, K.; Okano, T.; Sakurai, Y. *Advanced Drug Delivery Reviews* **1993**, 11, (1-2), 85-108.
3. Yoshida, R.; Takahashi, T.; Yamaguchi, T.; Ichijo, H. *Journal of the American Chemical Society* **1996**, 118, (21), 5134-5135.
4. Yoshida, R.; Yamaguchi, T.; Ichijo, H. *Materials Science & Engineering, C: Biomimetic Materials, Sensors and Systems* **1996**, C4, (2), 107-113.
5. Jones, R. A. L., *Soft Machines: Nanotechnology and Life*. Oxford University Press: **2004**.
6. Yoshida, R.; Sakai, T.; Ito, S.; Yamaguchi, T. *Journal of the American Chemical Society* **2002**, 124, (27), 8095-8098.
7. Burchard, W. *Advances in Polymer Science* **1999**, 143, 113-194.

8. Forster, S.; Konrad, M. *Journal of Materials Chemistry* **2003**, 13, (11), 2671-2688.
9. Leibler, L. *Macromolecules* **1980**, 13, (6), 1602-17.
10. Matsen, M. W.; Bates, F. S. *Macromolecules* **1996**, 29, (4), 1091-8.
11. Glatter, O.; Kratky, O.; Editors, *Small Angle X-ray Scattering*. **1982**; p 515 pp.
12. Cowie, J. M. G. 1991, 29.
13. Howse, J. R.; Topham, P.; Crook, C. J.; Gleeson, A. J.; Bras, W.; Jones, R. A. L.; Ryan, A. J. *Nano Letters* **2006**, 6, (1), 73-77.
14. Ryan, A. J.; Crook, C. J.; Howse, J. R.; Topham, P.; Jones, A. L.; Geoghegan, M.; Parnell, A. J.; Ruiz-Perez, L.; Martin, S. J.; Cadby, A.; Menelle, A.; Webster, J. R. P.; Gleeson, A. J.; Bras, W. *Faraday discussions* **2005**, 128, 55-74.
15. Edblom, E. C.; Luo, Y.; Orban, M.; Kustin, K.; Epstein, I. R. *Journal of Physical Chemistry* **1989**, 93, (7), 2722-7.
16. Crook, C. J.; Smith, A.; Jones, R. A. L.; Ryan, A. J. *Physical Chemistry Chemical Physics* **2002**, 4, (8), 1367-1369.
17. Niwa, M.; Higashizaki, T.; Higashi, N. *Tetrahedron* **2003**, 59, (22), 4011-4015.
18. Bashir, R.; Hilt, J. Z.; Elibol, O.; Gupta, A.; Peppas, N. A. *Applied Physics Letters* **2002**, 81, (16), 3091-3093.
19. Okazaki, N.; Rabai, G.; Hanazaki, I. *Journal of Physical Chemistry A* **1999**, 103, (50), 10915-10920.
20. Topham, P. D.; Howse, J. R.; Mykhaylyk, O. O.; Armes, S. P.; Jones, R. A. L.; Ryan, A. J. *Macromolecules* **2006**, 39, (16), 5573-5576.
21. Fairclough, J. P. A.; Salou, C. L. O.; Ryan, A. J.; Hamley, I. W.; Daniel, C.; Helsby, W. I.; Hall, C.; Lewis, R. A.; Gleeson, A. J.; Diakun, G. P.; Mant, G. R. *Polymer* **1999**, 41, (7), 2577-2582.
22. Bras, W.; Dolbnya, I. P.; Detollenaere, D.; van Tol, R.; Malfois, M.; Greaves, G. N.; Ryan, A. J.; Heeley, E. *Journal of Applied Crystallography* **2003**, 36, (3, Pt. 1), 791-794.
23. Bütin, V. *PhD Thesis; University of Sussex* **1999**, 18-28.
24. Simmons, M. R.; Yamasaki, E. N.; Patrickios, C. S. *Macromolecules* **2000**, 33, (8), 3176-3179.
25. Triftaridou, A. I.; Hadjiyannakou, S. C.; Vamvakaki, M.; Patrickios, C. S. *Macromolecules* **2002**, 35, (7), 2506-2513.
26. Topham, P. D.; Howse, J. R.; Crook, C. J.; Parnell, A. J.; Geoghegan, M.; Jones, R. A. L.; Ryan, A. J. *Polymer International* **2006**, 55, (7), 808-815.
27. Turro, N. J.; Caminati, G.; Kim, J. *Macromolecules* **1991**, 24, (14), 4054-60.
28. Bednar, B.; Trnena, J.; Svoboda, P.; Vajda, S.; Fidler, V.; Prochazka, K. *Macromolecules* **1991**, 24, (8), 2054-9.
29. Ogawa, Y.; Ogawa, K.; Kokufuta, E. *Langmuir* **2004**, 20, (7), 2546-2552.
30. Amalvy, J. I.; Wanless, E. J.; Li, Y.; Michailidou, V.; Armes, S. P.; Duccini, Y. *Langmuir* **2004**, 20, (21), 8992-8999.